

# A shotgun lipidomics approach in *Sinorhizobium meliloti* as a tool in functional genomics

Libia Saborido Basconcello,\* Rahat Zaheer,<sup>†</sup> Turlough M. Finan,<sup>†</sup> and Brian E. McCarry<sup>1,\*</sup>

Departments of Chemistry\* and Biology,<sup>†</sup> McMaster University, Hamilton, Ontario, Canada

**Abstract** A shotgun lipidomics approach that allowed the analysis of eight lipid classes directly from crude extracts of the soil bacterium *Sinorhizobium meliloti* is presented. New MS-MS transitions are reported for the analysis of monomethylphosphatidylethanolamines, dimethylphosphatidylethanolamines, and three bacterial non-phosphorus-containing lipid classes [sulfoquinovosyldiacylglycerols, ornithines, and diacylglyceryl-(*N,N,N*-trimethyl)-homoserines]. Unique MS-MS transitions allowed the analysis of isomeric species from various lipid classes without chromatography. Analyses required small sample amounts and minimal preparation; thus, this methodology has excellent potential to be used as a screening tool for the analysis of large numbers of samples in functional genomics studies. FA distributions within lipid classes of *S. meliloti* are described for the first time, and the relative positions of fatty acyl substituents (*sn*-1, *sn*-2) in phospholipids are presented. FA distributions in diacylglyceryl-(*N,N,N*-trimethyl)-homoserines were identical to those of phospholipids, indicating a common biosynthetic origin for these lipids. The method was applied to the analysis of mutants deficient in the PhoB regulator protein. Increased lipid cyclopropanation was observed in PhoB-deficient mutants under P<sub>i</sub> starvation.—Basconcello, L. S., R. Zaheer, T. M. Finan, and B. E. McCarry. A shotgun lipidomics approach in *Sinorhizobium meliloti* as a tool in functional genomics. *J. Lipid Res.* 2009. 50: 1120–1132.

**Supplementary key words** electrospray ionization • tandem mass spectrometry • sulfoquinovosyldiacylglycerol • diacylglyceryl-(*N,N,N*-trimethyl)-homoserine • ornithine • P<sub>i</sub> limitation • PhoB regulator

*Sinorhizobium meliloti* is a soil bacterium that transforms atmospheric nitrogen into a form utilizable by leguminous plants such as alfalfa while establishing a beneficial relationship in a process called nitrogen fixation (1, 2). The complete genome of *S. meliloti* has been annotated; however, the function of more than 40% of genes remains unknown (3, 4). In the past decade, numerous efforts have been directed toward understanding gene function (functional genomics) and the mechanisms by which symbiosis and nitrogen fixation occur (5–8). Our research focuses on the study of

genes in *S. meliloti* that are hypothesized to participate in lipid biosynthesis. Assignments of gene function have been made in most cases by comparing *S. meliloti*'s genome with the genomes of other well-studied organisms, such as *Escherichia coli*.

Comprehensive lipid profiling, also known as lipidomics, has been proposed as a strategy to improve our understanding of lipid metabolism and gene function (9–11). Our approach to understanding gene function employs comparisons of lipid and FA profiles of knockout mutants with those of wild-type strains. Thus, a rapid and comprehensive method for the analysis of lipids in *S. meliloti* was needed. Analytical methods for comprehensive lipid analysis must provide information regarding: *i*) lipid classes; *ii*) molecular species within lipid classes caused by variations of the fatty acyl chains; and *iii*) the relative locations of the fatty acyl chains in individual lipids (*sn*-1 vs. *sn*-2).

Typically, methods for intact lipid analysis involve lipid extraction followed by chromatographic separation of lipid classes and their detection by MS. TLC and HPLC (12, 13) are the most common chromatographic techniques, although capillary electrophoresis has also been employed (14). Two-dimensional high-performance TLC (2D-HPTLC) procedures have been used to separate crude lipid extracts into lipid classes (15). Obtaining FA distributions within each lipid class requires removal of TLC spots, extraction into an organic solvent, and analysis of the extract by electrospray mass spectrometry (ESI-MS) or GC-MS. TLC-based methodologies also suffer from losses due to lipid oxidation on the TLC plates, poor extraction recoveries from the silica gel, and slow throughput, making them inconvenient for high-throughput analyses (12, 16). On the other hand, HPLC-based methodologies separate lipids by classes or

Abbreviations: CE, collision energy; CID, collision-induced dissociation; CL, cardiolipin; DMPE, dimethylphosphatidylethanolamine; ESI-MS, electrospray mass spectrometry; FAME, fatty acid methyl ester; HPTLC, high-performance TLC; MMPE, monomethylphosphatidylethanolamine; NP, normal phase; OL, ornithine lipid; PC, phosphatidylcholine; PCA, principal components analysis; PE, phosphatidylethanolamine; PG, phosphatidylglycerol; PHB, poly(3-hydroxybutyrate); P<sub>i</sub>, inorganic phosphate; RP, reverse phase; SL, sulfoquinovosyldiacylglycerol; TMHS, 1,2-diacylglyceryl-3-O-4'-(*N,N,N*-trimethyl)-homoserine lipid.

<sup>1</sup>To whom correspondence should be addressed.

e-mail: mccarry@mcmaster.ca

Manuscript received 19 August 2008 and in revised form 11 December 2008.

Published, JLR Papers in Press, December 18, 2008.

DOI 10.1194/jlr.M800443-JLR200

into their molecular constituents using normal-phase HPLC (NP-HPLC) or reverse-phase HPLC (RP-HPLC), respectively (12). When complete chromatographic separation of both lipid classes and their individual molecular species is desired, a combination of NP-HPLC followed by RP-HPLC has been applied (13, 17, 18). The separation of isomeric species of different lipid classes and chromatographic co-elution present major analytical challenges (12).

Chromatographic procedures for intact lipid analysis tend to be laborious; moreover, chromatographic methods often suffer from poor lipid recoveries and changes to the distribution of molecular species (16). While HPLC-ESI-MS analysis is currently the most common approach in lipid analysis, Han and Gross (19) demonstrated that phospholipids can be analyzed directly by the infusion of crude lipid extracts under ESI conditions; this approach has been termed "shotgun lipidomics." Shotgun lipidomics uses a combination of MS-MS techniques to differentiate lipid classes by their fragmentation patterns under collision-induced dissociation (CID) (20, 21). This methodology requires small sample amounts and minimal sample preparation, features well suited to functional genomics applications. Tandem mass spectrometric analyses of lipids can provide information regarding not only the nature of the fatty acyl chains but also their relative positions (*sn*-1 vs. *sn*-2) in individual lipids (22–24). Therefore, we sought to develop a shotgun lipidomics procedure for the analysis of intact lipids in crude extracts of *S. meliloti* as a tool for functional genomics studies. Although analyses of intact lipids in *S. meliloti* have been reported using TLC procedures, FA distributions within lipid classes and the location of FAs in lipids (*sn*-1 vs. *sn*-2) have not been reported in *S. meliloti*.

Cell membranes in *S. meliloti* are composed of phospholipids that include phosphatidylcholines (PCs, ~60%), phosphatidylethanolamines and monomethylphosphatidylethanolamines (PEs + MMPEs, ~20%), dimethylphosphatidylethanolamines (DMPEs, ~2%), phosphatidylglycerols (PGs, ~9%), and cardiolipins (CLs, ~5%) (25). Non-phosphorus-containing lipids such as sulfoquinovosyldiacylglycerols (SLs) and ornithine lipids (OLs) are also present but comprise less than 5% of total lipids under normal growth conditions (25). Under inorganic phosphate ( $P_i$ )-limiting conditions, non-phosphorus-containing lipids [SLs, OLs, and 1,2-diacylglycerol-3-*O*-4'-(*N,N,N*-trimethyl)-homoserine lipids (TMHSs)] become the major membrane components, often representing up to 70% of total lipids (25). Shotgun lipidomics approaches have been developed for the analysis of lipids encountered in eukaryotic cells (phospholipids and sphingolipids). However, there are no reports of the use of this approach for the analysis of bacterial lipids such as MMPEs, DMPEs, SLs, TMHSs, or OLs. Therefore, major goals of this work were to develop a shotgun lipidomics method suitable for the analysis of minor lipids such as MMPEs, DMPEs, and non-phosphorus-containing lipids in *S. meliloti* and to provide detailed FA distributions within each of these lipid classes. These FA data were to be compared with the overall FA profile obtained for the crude lipid fraction. In order to test the value of our approach, the methodology was used to exam-

ine changes in the lipidome of *S. meliloti* (both intact lipids and FAs) under two different scenarios: in phosphate-containing ( $P_i$ ) and  $P_i$ -limiting conditions using a wild-type strain and a *phoB* mutant strain. *PhoB* was selected because it is a well-studied global regulator known to modulate the expression of genes during stress induced in the bacterium by low levels of phosphate (8, 26).

## EXPERIMENTAL PROCEDURES

### Reagents

*N*-methyl-*N*-(trimethylsilyl)trifluoroacetamide and ethyl dodecanoate were obtained from Sigma-Aldrich (St. Louis, MO). All solvents used were HPLC grade (Caledon Labs, Caledon, ON). Phospholipid standards, 1,2-diheneicosanoyl-*sn*-glycero-3-phosphocholine [PC(21:0/21:0)], 1,2-dimyristoyl-*sn*-glycero-3-phosphoethanolamine [(PE(14:0/14:0)], and 1,2-dilauroyl-*sn*-glycero-3-phospho-*rac*-(1-glycerol) [(PG(12:0/12:0), sodium salt] were purchased from Avanti Polar Lipids (Alabaster, AL).

### Bacterial strains and growth conditions

Wild-type *S. meliloti* (RmP110) and *phoB* mutant RmH838 containing *phoB3::Tn5* (27) were grown in MOPS-buffered minimal media (28) containing 10 ng/ml  $CoCl_2$ , 0.5  $\mu$ g/ml biotin, and glucose (15 mM) as the carbon source in the presence (2 mM) or absence of  $P_i$ . Wet cell pellets obtained from 500 ml of culture (Optical Density = 0.3–0.6) by centrifugation were resuspended in 2.5 ml of MOPS medium with no phosphate present and divided into 250  $\mu$ l aliquots in microfuge tubes (equivalent to 50 ml of original cell culture). Each tube was then centrifuged, the supernatant was discarded, and the wet pellets were stored at  $-80^\circ C$  following flash freezing in liquid nitrogen. The wet pellets (equivalent to 50 ml of culture) with 2 mM  $P_i$  and without  $P_i$ , weighed  $32.7 \pm 2.3$  mg ( $n = 6$ ) or  $20.9 \pm 3.1$  mg ( $n = 6$ ), respectively.

### Lipid extraction

Wet cell pellets (equivalent to 50 ml of bacterial culture) were resuspended in distilled water (1 ml) and extracted with a mixture of  $CHCl_3$ -MeOH (1 ml, 2:1, v/v). The  $CHCl_3$  phase containing the lipids was separated, and the aqueous phase was extracted twice more with  $CHCl_3$ -MeOH (1 ml, 2:1, v/v). The chloroform phases from each extraction were pooled and dried through a small column packed with anhydrous sodium sulfate (~1 g). The eluent was evaporated using a stream of nitrogen gas, and the dried lipid residue was either analyzed immediately or stored at  $-80^\circ C$ .

### Fatty acid methyl ester analysis by GC-MS

FAs in crude lipid extracts were analyzed as their fatty acid methyl esters (FAMES) by GC-MS. FAMES were prepared from dried lipid extracts using a one-vial method that employed sodium methoxide in methanol as the transmethylation reagent (29).

### Chromatography

Dried lipid extracts (corresponding to 50 ml of bacterial culture) were dissolved in  $CHCl_3$ -MeOH (100  $\mu$ l, 1:1, v/v) and applied to columns packed with silica gel (1 g, 35–75  $\mu$ m). Glycolipids were eluted with acetone as described by Christie (15). The fraction containing the glycolipids was dried under nitrogen stream and stored at  $-80^\circ C$  for mass spectrometric analysis.

## MS

Dried lipid extracts obtained from 50 ml of bacterial culture were dissolved in 200  $\mu$ l MeOH-CHCl<sub>3</sub> (1:1, v/v). For analyses in the positive-ionization mode, aliquots (20  $\mu$ l) were diluted 5-fold with MeOH (80  $\mu$ l) containing PC(21:0/21:0) (32  $\mu$ mol), PE(14:0/14:0) (28  $\mu$ mol), and lithium chloride (2.5 mM). For analyses in the negative-ion mode, aliquots (20  $\mu$ l) of the lipid extract were diluted 5-fold with methanol (80  $\mu$ l) containing PG (12:0/12:0) (3  $\mu$ mol) as the internal standard. A Waters Quattro Ultima triple quadrupole mass spectrometer equipped with a microelectrospray ionization source and operating under the MassLynx software was used for the analysis of bacterial lipid extracts. The collision gas (N<sub>2</sub>) pressure was  $2 \times 10^{-3}$ . Bar and collision energies (CEs) ranged between 25 eV and 50 eV. Lipid extracts were continuously infused at 1  $\mu$ l/min using a Harvard syringe pump.

PCs, DMPEs, MMPEs, and PEs were simultaneously analyzed as their lithiated adducts in the positive-ionization mode using neutral-loss scans of 189 (30), 175, 161, and 147 (22) mass units with a CE of 35 eV. TMHSs and OLs were also analyzed as [M+Li]<sup>+</sup> ions using neutral-loss scan of 74 mass units (CE 40 eV) and precursor ion scan of *m/z* 115 (CE 35 eV), respectively. PGs and SLs were analyzed as their [M-H]<sup>-</sup> ions in the negative-ionization mode, using precursor ion scans of *m/z* 153 (21, 31) and 225, respectively (CE 50 eV). One hundred mass spectra were averaged in each mass spectrometry experiment. Peak areas obtained from each MS-MS spectrum were corrected for the <sup>13</sup>C isotope effect when the pseudomolecular ion peak overlapped with the M+2 isotopic peak of other lipids (21), then normalized using the peak area of an internal standard. Relative percentage compositions of

individual lipid species were obtained for each lipid class using the peak areas normalized to the internal standard in precursor ion or neutral-loss spectra.

High-resolution mass spectra were obtained using a Global Ultima Quadrupole Time of Flight Mass Spectrometer (Waters, Manchester, UK). Lipid extracts (CHCl<sub>3</sub>-MeOH, 1:1, v/v) were infused continuously (1–5  $\mu$ l/min) via a microelectrospray ionization source. Argon was used as the collision gas.

## Statistical analyses

All data are reported as mean values  $\pm$  standard deviation. A statistical package (SPSS, version 15.0; SPSS, Inc., Chicago, IL) was used for statistical analyses. Student's *t*-test was used (*P*  $\leq$  0.05) to evaluate two groups of data. Principal component analyses (PCAs) were performed using the SPSS software and the Multivariate Analysis Add-in for Excel, version 1.3 (Bristol Chemometrics, Inc., Bristol, UK).

## RESULTS

### Analysis of PGs: FA substituents, and their relative positions in lipids

A typical profile of a crude lipid extract of *S. meliloti* in negative electrospray ionization in the full-scan mode is presented in Fig. 1A. An internal standard, PG(12:0/12:0), was added to lipid mixtures. The full-scan mode spectrum showed [M-H]<sup>-</sup> ions corresponding to nine PGs, with major

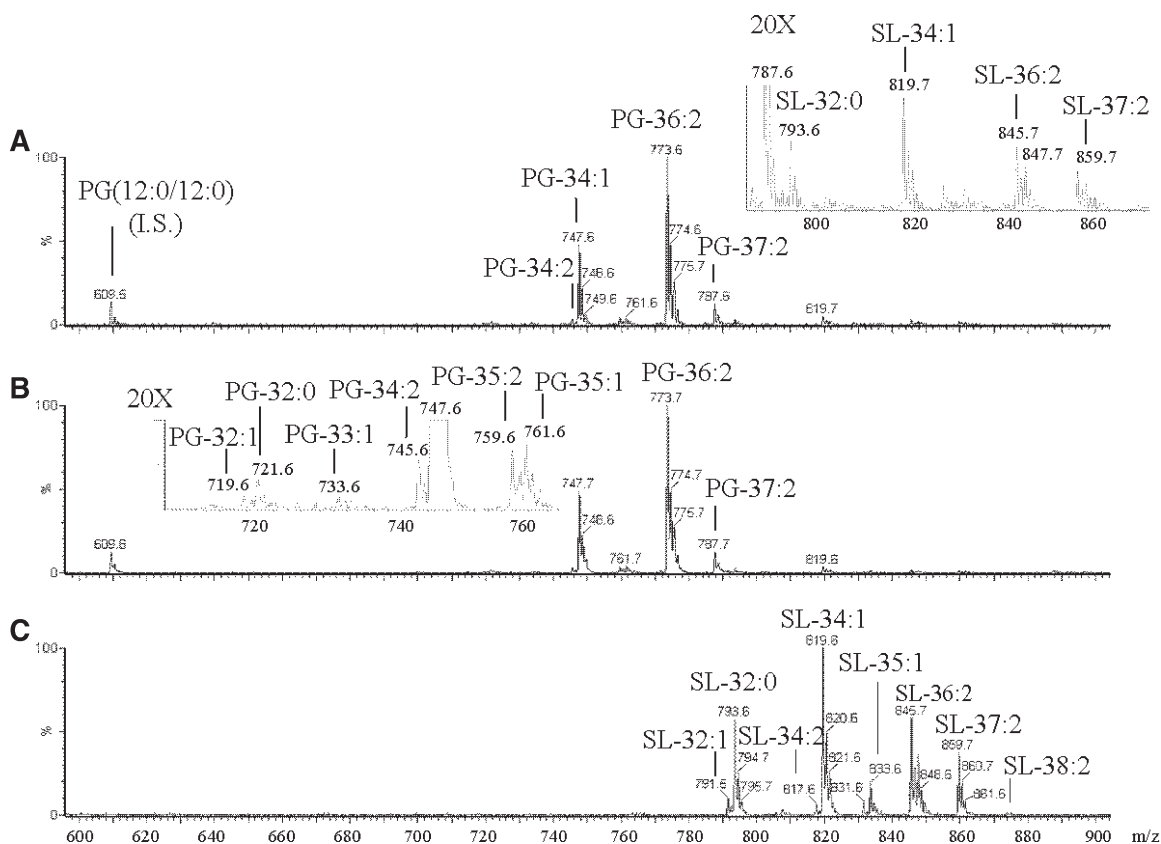


**Fig. 1.** Electrospray ionization mass spectra in the negative-ionization mode of crude lipid extracts of *Sinorhizobium meliloti* P110 grown in MOPS medium. A: Full-scan mode; insert shows an expanded view of *m/z* 700–760. B: Precursor ion scan of *m/z* 153. C: Precursor ion scan of *m/z* 225. I.S., internal standard; PG, phosphatidylglycerol; SL, sulfoquinovosyldiacylglycerol.

ions at  $m/z$  747.6, 773.6, and 787.6. In addition, other minor peaks that corresponded to four SLs were detected. The CID spectra of the nine PGs ( $m/z$  719.5, 721.5, 745.5, 747.5, 759.5, 761.5, 773.5, 787.5, and 801.6) afforded product ion spectra typical of PGs. All mass spectra showed fragment ions corresponding to carboxylate ions due to losses of the fatty acyl substituents and a weak ion at  $m/z$  153 corresponding to the polar head group,  $[\text{HO}_3\text{POCH}_2\text{C}(\text{OH})\text{CH}_2]^-$  (31). These  $m/z$  values were identified as  $[\text{M}-\text{H}]^-$  ions of PGs with FA compositions corresponding to PG-32:1, PG-32:0, PG-34:2, PG-34:1, PG-35:2, PG-35:1, PG-36:2, PG-37:2, and PG-38:2, respectively.

Upon CID,  $[\text{M}-\text{H}]^-$  ions of PGs typically produce  $[\text{RCOO}]^-$  ions from the loss of FAs in the  $sn$ -2 position, which are more abundant than  $[\text{RCOO}]^-$  ions originated from losses of FAs in the  $sn$ -1 position (23). Thus, this feature of the product ion spectra of PGs was used to determine the nature of the fatty acyl chains and their relative positions (Table 1). Previous studies of total FA composition in *S. meliloti* by GC-MS analysis (29) greatly facilitated the identification of possible FA combinations for each lipid. The product ion spectra of anionic lipids that contain nonadecenoic acid (19:1) or methyleneoctadecanoic acid (19:0cyclo) yield a  $[\text{RCOO}]^-$  ion at  $m/z$  295.2637, with the same elemental composition of  $\text{C}_{19}\text{H}_{35}\text{O}_2$ . GC-MS analysis determined that *S. meliloti* contained methyleneoctadecanoic acid and not nonadecenoic acid (29). The assignments of FAs to the  $sn$ -1 or  $sn$ -2 position for some minor lipids were ambiguous.

Precursor ion scans of  $m/z$  153 were used to provide complete profiles of PGs in crude lipid extracts of *S. meliloti* (Fig. 1B). Upon CID fragmentation of  $[\text{PG}-\text{H}]^-$  ions, the polar head group ion at  $m/z$  153 was of low abundance. To improve the sensitivity of this MS-MS transition, precursor ion scans of  $m/z$  153 were conducted at CE of 50 eV. In addition, 100 spectra were routinely collected to improve

the S/N ratios, especially for minor PGs; detection limits were in the low picomole range [0.5 pmol/ $\mu\text{l}$  for PG(12:0/12:0)]. Although other researchers have also employed precursor ion scans of  $m/z$  153 to profile PGs in crude lipid extracts (21), most methodologies employ chromatographic separations (32–34). We believe that precursor ion scan of  $m/z$  153 is a simpler and faster strategy to profile PGs in bacterial extracts in comparison with chromatographic methods.

#### Analysis of PCs, PEs, MMPEs, and DMPEs: FA substituents and their relative positions in lipids

PCs and PEs were detected as a mixture of  $[\text{M}+\text{H}]^+$  and  $[\text{M}+\text{Na}]^+$  ions upon infusion of crude extracts in positive electrospray ionization conditions (Fig. 2A). Under CID conditions, the product ion spectra of  $[\text{M}+\text{H}]^+$  adducts of PCs and PEs showed fragments typical of the polar head groups at  $m/z$  184 ( $[\text{H}_2\text{PO}_4(\text{CH}_2)_2\text{N}(\text{CH}_3)_3]^+$ ) for PCs, or a neutral loss of 141 mass units ( $[(\text{OH})_2(\text{PO})\text{OCH}_2\text{CH}_2\text{NH}_2]^+$ ) for PEs (31, 35). The CID spectra of  $[\text{M}+\text{H}]^+$  and  $[\text{M}+\text{Na}]^+$  ions of PCs and PEs are rather uninformative regarding the nature and position of the fatty acyl substituents in lipids (30). Table 2 shows the  $m/z$  values of  $[\text{M}+\text{H}]^+$  and  $[\text{M}+\text{Na}]^+$  adducts formed by PCs and PEs of various FA compositions detected in *S. meliloti*.

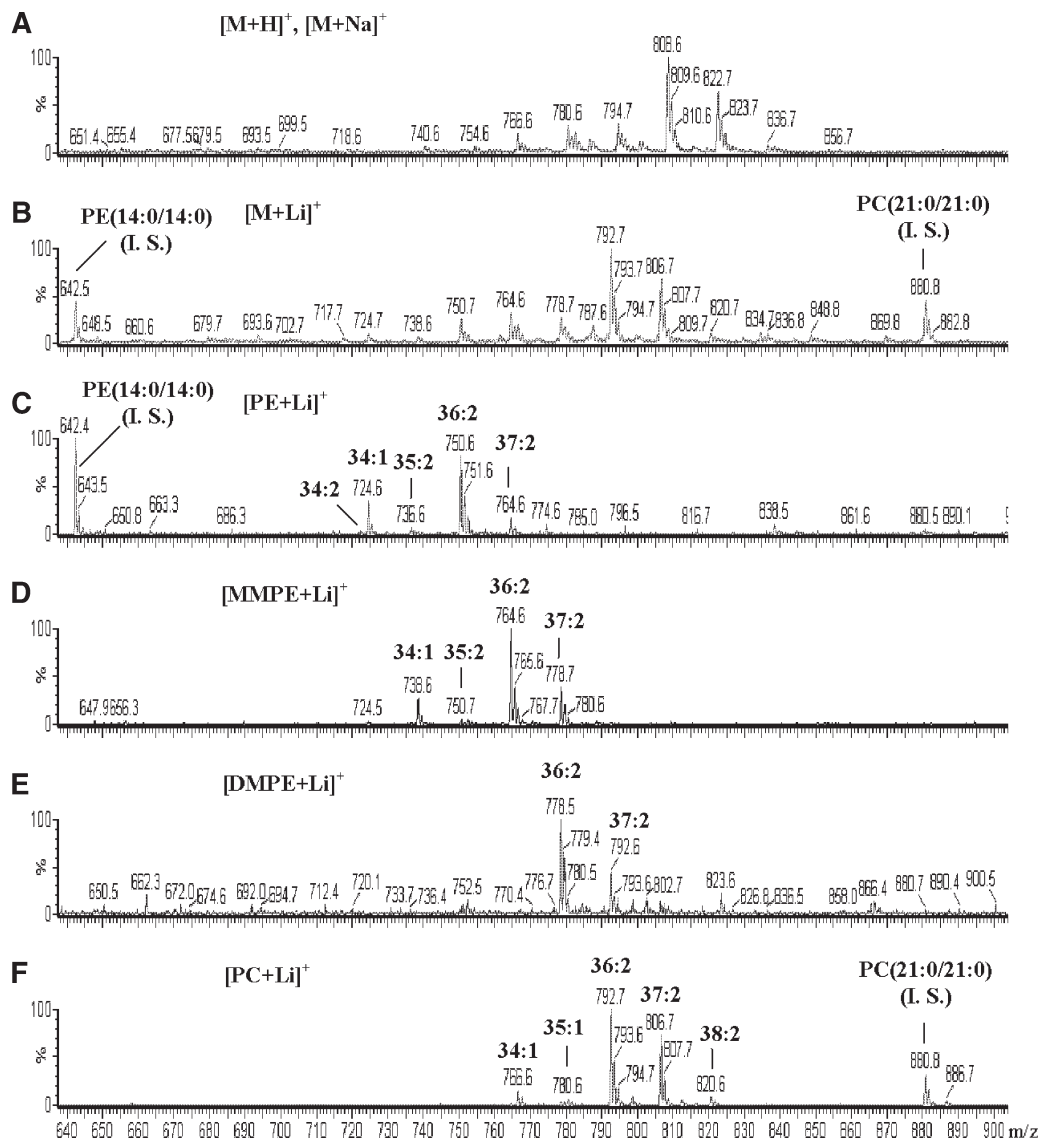
In the presence of lithium salts, PCs and PEs form  $[\text{M}+\text{Li}]^+$  ions, which upon CID, produce product ion spectra that contain diagnostic fragment ions for both the polar head group and the fatty acyl groups (22, 24, 30). The lipid profiles of extracts of *S. meliloti* in the positive-ionization mode in the presence of lithium salts are shown in Fig. 2B; two internal standards were included, PC(21:0/21:0) and PE (14:0/14:0). The addition of lithium significantly simplified lipid profiles by converting the mixture of  $[\text{M}+\text{H}]^+$  and  $[\text{M}+\text{Na}]^+$  ions to  $[\text{M}+\text{Li}]^+$  ions. This can be appreciated

TABLE 1. Fatty acyl chains and their relative positions ( $sn$ -1/ $sn$ -2) in individual lipids in four lipid classes in *Sinorhizobium meliloti*

Lipid	Fatty Acyl Chains in Lipids $sn$ -1/ $sn$ -2			
	PG	SL	PC	OL
32:1	16:1-16:0	16:1-16:0		
32:0	16:0/16:0	16:0/16:0		
33:1	16:0/17:0cyclo			
33:0	17:0-16:0			
34:2	18:1/16:1	18:1-16:1	16:1/18:1	
34:1	18:1/16:0	18:1-16:0	18:1/16:0	3OH-16:0/18:1 <sup>a</sup> 3OH-18:0/16:1 <sup>a</sup>
35:2	18:1/17:0cyclo	18:1-17:0cyclo	18:1/17:0cyclo	
	16:1-19:0cyclo	16:1-19:0cyclo	16:1-19:0cyclo	
35:1	19:0cyclo/16:0	19:0cyclo-16:0	19:0cyclo/16:0	3OH-16:0/19:0cyclo <sup>a</sup> 3OH-18:0/17:0cyclo <sup>a</sup> 3OH-16:0/22:2 <sup>a</sup> 3OH-18:0/18:2 <sup>a</sup> 3OH-18:0/18:1
36:2	18:1/18:1	18:1/18:1	18:1/18:1	3OH-18:1/19:0cyclo <sup>a</sup> 3OH-18:0/19:0cyclo 3OH-18:0/20:2 <sup>a</sup> 3OH-18:0/21:2 <sup>a</sup>
36:1		18:1-18:0		
37:2	19:0cyclo/18:1	19:0cyclo-18:1	19:0cyclo/18:1	
37:1				
38:2	19:0cyclo/19:0cyclo	19:0cyclo/19:0cyclo	19:0cyclo/19:0cyclo	
39:2				

FAs are separated by a hyphen when their assignment to the  $sn$ -1 and  $sn$ -2 positions was ambiguous. OL, ornithine lipid; PC, phosphatidylcholine; PG, phosphatidylglycerol; SL, sulfoquinovosyldiacylglycerol.

<sup>a</sup> Possible FA combinations for ornithine lipids.



**Fig. 2.** Electrospray ionization mass spectra in the positive-ion mode of crude lipid extracts of *S. meliloti* P110. A: Full-scan mode. B: Full-scan mode, 10 mM LiCl added. C: Neutral-loss scan of 147 mass units. D: Neutral-loss scan of 161 mass units. E: Neutral-loss scan of 175 mass units. F: Neutral-loss scan of 189 mass units. DMPE, di-methylphosphatidylethanolamine; MMPE, monomethylphosphatidylethanolamine; PC, phosphatidylcholine; PE, phosphatidylethanolamine.

when comparing the high number of lipid adducts detected in crude extracts (Table 2), relative to the significantly reduced number of species detected when  $\text{Li}^+$  was added (Table 3).

Product ion spectra of  $[\text{PC}+\text{Li}]^+$  contained unique fragment ions at  $m/z$   $[\text{PC}+\text{Li}-59]^+$  and  $[\text{PC}+\text{Li}-189]^+$  due to neutral losses of  $\text{N}(\text{CH}_3)_3$  and  $[\text{N}(\text{CH}_3)_3+\text{LiOPO}_3(\text{CH}_2)_2]$ , respectively (24). Fatty acyl groups in lipids were determined using fragment ions at  $m/z$   $[\text{PC}+\text{Li}-59-\text{RCOOH}]^+$ , whereas their relative positions in the glycerol backbone (*sn*-1, *sn*-2) were determined by their intensities, because fragment ions originated from the loss of FAs in *sn*-1 are more intense than those of the *sn*-2 position (24, 30). The fatty acyl chains and their relative positions in lipids (*sn*-1 and *sn*-2) are listed in Table 1. Similarly, product ion spectra of  $[\text{PE}+\text{Li}]^+$  adducts afforded fragment ions of the types

$[\text{PE}+\text{Li}-43]^+$  and  $[\text{PE}+\text{Li}-147]^+$ , characteristic of the polar head group of PEs (22). Fragment ions at  $m/z$   $[\text{PE}+\text{Li}-43-\text{RCOOH}]^+$  determine fatty acyl groups, and their relative positions in lipids is given by their relative intensities (*sn*-1 > *sn*-2) (22). Neutral-loss scans of 189 and 147 mass units, corresponding to the losses of the lithiated polar head groups of PCs and PEs respectively, afforded individual profiles for each lipid class (Fig. 2B, F). Lipid analysis methodologies commonly require either TLC or NP-HPLC followed by RP-HPLC in order to eliminate the coelution of isomeric species of PCs and PEs with various FA compositions (18).

MMPEs and DMPEs are typically analyzed using TLC-based methodologies (25). Upon lithium addition to lipid extracts, MMPEs and DMPEs were detected as  $[\text{M}+\text{Li}]^+$ , given their chemical structures similar to those of PEs. The characteristic fragment ion of lithiated PEs at  $m/z$

TABLE 2. Nominal  $m/z$  values for  $[M+H]^+$  and  $[M+Na]^+$  adduct ions of PEs, MMPEs, DMPEs, PCs, and TMHSs species observed in lipid extracts of *S. meliloti*

$m/z$		$[M+H]^+$	$[M+Na]^+$
716.5	PE-34:2		
718.5	PE-34:1		
730.5	PE-35:2+ MMPE-34:2		
732.6	PE-35:1+ MMPE-34:1		
736.6	TMHS-34:2		
738.5 <sup>a</sup>			PE-34:2
738.6 <sup>a</sup>	TMHS-34:1		
740.5			PE-34:1
744.6	PE-36:2+ MMPE-35:2+ DMPE-34:2		
746.6	MMPE-35:1+ DMPE-34:1		
750.6	TMHS-35:2		
752.5 <sup>a</sup>			PE-35:2+ MMPE-34:2
752.6 <sup>a</sup>	TMHS-35:1		
754.5			PE-35:1+ MMPE-34:1
758.6	PE-37:2+ MMPE-36:2+ DMPE-35:2+ PC-34:2 (758.5700) <sup>b</sup>		TMHS-34:2 (758.5911) <sup>b</sup>
760.6	DMPE-35:1+ PC-34:1 (760.5856) <sup>b</sup>		TMHS-34:1 (760.6067) <sup>b</sup>
764.6	TMHS-36:2		
766.5			PE-36:2+ MMPE-35:2+ DMPE-34:2
768.6			MMPE-35:1+ DMPE-34:1
772.6	PE-38:2+ MMPE-37:2+ DMPE-36:2+ PC-35:2 (772.5856) <sup>b</sup>		TMHS-35:2 (772.6067) <sup>b</sup>
774.6	PC-35:1 (774.6013) <sup>b</sup>		TMHS-35:1 (774.6224) <sup>b</sup>
778.7	TMHS-37:2		
780.6			PE-37:2+ MMPE-36:2+ DMPE-35:2+ PC-34:2
782.6			MMPE-36:1+ DMPE-35:1+ PC-34:1
786.6	MMPE-38:2+ DMPE-37:2+ PC-36:2 (786.6013) <sup>b</sup>		TMHS-36:2 (786.6224) <sup>b</sup>
792.6	TMHS-38:2		
794.6			PE-38:2+ MMPE-37:2+ DMPE-36:2+ PC-35:2
796.6			PC-35:1
800.6	DMPE-38:2+ PC-37:2 (800.6169) <sup>b</sup>		TMHS-37:2 (800.6380) <sup>b</sup>
808.6			MMPE-38:2+ DMPE-37:2+ PC-36:2
814.6	PC-38:2 (814.6326) <sup>b</sup>		TMHS-38:2 (814.6537) <sup>b</sup>
822.6			DMPE-38:2+ PC-37:2
836.6			PC-38:2

MMPE, monomethylphosphatidylethanolamine; DMPE, dimethylphosphatidylethanolamine; TMHS, 1,2-diacylglycerol-3-O-4'-(*N,N,N*-trimethyl)-homoserine lipid. Accurate mass values for lipid adduct ions with the same nominal  $m/z$  value are included in brackets.

<sup>a</sup> Resolution of  $[M+H]^+$  and  $[M+Na]^+$  adducts with the same nominal mass value would require mass resolutions of  $\sim 6,300$ .

<sup>b</sup> Resolution of  $[M+H]^+$  and  $[M+Na]^+$  adducts with the same nominal mass value would require mass resolutions of  $\sim 39,000$ .

$[PE+Li-147]^+$  originates due to the sequential neutral losses of  $HN(CH_2)_2$  and  $LiOP(O)(OH)_2$  (22). Under CID conditions, the lithiated adducts of MMPEs and DMPEs fragmented similarly to  $[PE+Li]^+$ , a logical result given their chemical structures.  $[MMPE+Li]^+$  and  $[DMPE+Li]^+$  afforded unique fragment ions at  $m/z$   $[MMPE+Li-161]^+$  and  $[DMPE+Li-175]^+$ , respectively. Most likely, these neutral losses were the result of sequential losses of  $[CH_3N(CH_2)_2+LiOP(O)(OH)_2]$  and  $[CH_3N(CH_2)_3+LiOP(O)(OH)_2]$ , respectively. Thus, neutral losses of 161 and 175 mass units can be related to the lithiated polar head groups of MMPEs and DMPEs, respectively. Unfortunately, analytical standards of MMPEs and DMPEs are not commercially available to confirm these MS-MS transitions. Neutral-loss scans of 141 and 175 mass units afforded complete lipid profiles of lithiated MMPEs and DMPEs, respectively (Fig. 2D, E).

Isomeric species of MMPEs, DMPEs, PEs, and PCs of various FA compositions were present in *S. meliloti* [e.g., PC-35:2, DMPE-36:2, MMPE-37:2, and PE-38:2 at  $m/z$  778.6 (Table 3)]. Isomeric species cannot be differentiated using high mass resolution MS; additionally, the analysis of isomeric species of PEs, MMPEs, and DMPEs based on chromatographic separation would be challenging. The use of unique MS-MS transitions for lithiated PCs, PEs,

MMPEs, and DMPEs originated from differences in their polar head groups provided FA distributions within each lipid class without the need for chromatography.

#### Analysis of bacterial non-phosphorus-containing lipids: SLs, TMHSs, and OLS

SLs were readily detected as  $[M-H]^-$  ions in negative electrospray ionization when crude lipid extracts were infused (Fig. 1A, insert). The most abundant molecular species corresponded to SL-32:0, SL-34:1, SL-36:2, and SL-37:2 detected at  $m/z$  793.6, 819.7, 845.7, and 859.7, respectively. Product ion spectra of these ions afforded  $[RCOO]^-$  ions that matched SLs with FA combinations of 16:0/16:0, 18:1/16:0, 18:1/18:1, and 19:0cyclo/18:1 for SL-32:0, SL-34:1, SL-36:2, and SL-37:2, respectively. Additionally, the product ion spectra of all SLs afforded a fragment ion at  $m/z$  225.0. When Cedergren and Hollingsworth (36) characterized SLs in *S. meliloti* for the first time, they reported a fragment ion at  $m/z$  225.0, identified as the dehydrosulfolipid anion. To confirm that these ions corresponded to SLs, we prepared a glycolipid fraction from lipid extracts using silica gel flash chromatography (15); glycolipid fractions were analyzed using a triple quadrupole mass spectrometer and a quadrupole-time-of-flight tandem mass spectrometer. Accurate mass measurements of fragment

TABLE 3. Nominal  $m/z$  values for  $[M+Li]^+$  adducts of lipid species observed in *S. meliloti*

$m/z$	Lipids Observed as Their $[M+Li]^+$ Adducts				
	NL 74	NL 147	NL 161	NL 175	NL 189
722.5		PE-34:2			
724.5		PE-34:1			
736.5 <sup>a</sup>		PE-35:2	MMPE-34:2		
738.6 <sup>a</sup>		PE-35:1	MMPE-34:1		
742.6	TMHS-34:2				
744.6	TMHS-34:1				
750.6 <sup>a</sup>		PE-36:2	MMPE-35:2	DMPE-34:2	
752.6 <sup>a</sup>			MMPE-35:1	DMPE-34:1	
756.6	TMHS-35:2				
758.6	TMHS-35:1				
764.6 <sup>a</sup>		PE-37:2	MMPE-36:2	DMPE-35:2	PC-34:2
766.6 <sup>a</sup>				DMPE-35:1	PC-34:1
770.6	TMHS-36:2				
778.6 <sup>a</sup>		PE-38:2	MMPE-37:2	DMPE-36:2	PC-35:2
780.6					PC-35:1
784.7	TMHS-37:2				
792.6 <sup>a</sup>			MMPE-38:2	DMPE-37:2	PC-36:2
798.7	TMHS-38:2				
806.6 <sup>a</sup>				DMPE-38:2	PC-37:2
820.6					PC-38:2

<sup>a</sup> Isomeric species of different lipid classes were detected using neutral-loss scans unique to each lipid class.

ions at  $m/z$  80.9655 and 225.0076 in the product ion spectra of  $[M-H]^-$  ions of major SLs confirmed elemental compositions of  $HSO_3$  (80.9655) and  $C_6H_9O_7S$  (225.0076), respectively. These fragment ions are typical of SLs, and therefore these peaks were identified as SLs (36, 37). Precursor ion scans of  $m/z$  225.0 provided profiles of SLs directly from crude lipid extracts of *S. meliloti*; 10 molecular SL species were detected (Fig. 1C). To improve the S/N ratios, CEs of 50 eV were used to favor fragmentation of  $[M-H]^-$  ions, and 100 spectra were averaged.

OLs contain two amino functions and one carboxylic group; thus  $[M-H]^-$ ,  $[M+H]^+$ , or  $[M+Na]^+$  ions can be observed in electrospray ionization. Geiger and coworkers (25) isolated OLs from lipid extracts of *S. meliloti* using an HPTLC-based method; two OLs were detected as  $[M+H]^+$  ions at  $m/z$  679 and 693, which contained 3-hydroxyoctadecanoic acid with the hydroxyl group esterified to octadecenoic acid or methyleneoctadecanoic acid, respectively (25, 38). The product ion spectra of protonated ornithines typically contain an abundant fragment ion at  $m/z$  115, which is characteristic of ornithine-containing lipids (25, 38, 39). In this study, when crude lipid extracts of *S. meliloti* were directly infused, we detected peaks of low-abundance ions at  $m/z$  679.4 and 693.5 (Fig. 3A, B). The product ion spectra of these peaks contained abundant fragment ions at  $m/z$  115; thus peaks at  $m/z$  679.4 and 693.5 were identified as OLs.

Because a fragment ion at  $m/z$  115 is common to the MS-MS spectra of OLs, we employed precursor ion scans of  $m/z$  115 to investigate crude lipid extracts (Fig. 3D). In addition to the major OLs at  $m/z$  679.7 and 693.7 identified by Geiger, we detected another six OLs at  $m/z$  651.7, 665.7, 677.7, 691.7, 705.6, and 719.9. These ions corresponded to protonated OLs with FA compositions of 34:1, 35:1, 36:2, 37:2, 38:2, and 39:2. The FA compositions of

low-abundance OLs could not be determined, because these ions were only observed in precursor ion spectra. Because three hydroxy FAs (3-hydroxytetradecanoic acid, 3-hydroxyhexadecanoic acid, and 3-hydroxyoctadecanoic acid) (29) can be found in *S. meliloti*, these OLs could be amides of either of these 3-hydroxy FAs. For example, peaks at  $m/z$  651.7 (OL-34:1) and 665.7 (OL-35:1) could correspond to amides of 3-hydroxyhexadecanoic acid with the hydroxyl function esterified to 18:1 and 19:0cyclo, respectively. However, these OLs could also possibly be amides of 3-hydroxyoctadecanoic acid with the hydroxyl function esterified to 16:1 (OL-34:1) and 17:0cyclo (OL-35:1) FAs, respectively. OLs at  $m/z$  705.6 (OL-38:2) and 719.9 (OL-39:2) most likely are amides of 3-hydroxyoctadecanoic with FAs 20:2 and 21:2, respectively (Table 1).

TMHSs are ether-linked glycerolipids with a quaternary ammonium group that resemble PCs (40). TMHSs can be detected as mixtures of  $[M+H]^+$  or  $[M+Na]^+$  ions similarly to PCs and PEs in positive electrospray ionization. Geiger and coworkers, using a TLC-based procedure, detected two TMHSs in lipid extracts of *S. meliloti* as their  $[M+H]^+$  ions at  $m/z$  764 and 778; these lipids were identified as TMHS-36:2 and TMHS-37:2, respectively (25, 41). When crude lipid extracts of *S. meliloti* grown under P<sub>1</sub> starvation were directly infused,  $[M+H]^+$  ions at  $m/z$  764 and 778 for TMHS-36:2 and TMHS-37:2, respectively, were not detected (Fig. 3A). However, other peaks were detected at the expected  $m/z$  values for the  $[M+Na]^+$  adducts of TMHS-36:2 ( $m/z$  786.6) and TMHS-37:2 ( $m/z$  800.5) (Table 2 and Fig. 3A). Ions at  $m/z$  786.6 and 800.5 could also correspond to  $[M+H]^+$  adducts of PC-36:2, DMPE-37:2, MMPE-38:3, PC-37:2, and DMPE-38:2 lipids, which were also detected in lipid extracts of *S. meliloti* (Table 2). If TMHSs exhibited FA distributions similar to those observed in phospholipids (PCs, PEs, etc.), then considerable mass overlap would occur due to the coexistence of  $[M+H]^+$  and  $[M+Na]^+$  ions (Table 2). Note that mass resolutions of up to 38,600 would be required to resolve  $[M+H]^+$  and  $[M+Na]^+$  ions of [PCs+PEs+MMPEs+DMPEs] and TMHSs.

Upon addition of lithium to lipid extracts, peaks were detected at the expected  $m/z$  values of  $[M+Li]^+$  adducts of TMHS-36:2 ( $m/z$  770.7) and TMHS-37:2 ( $m/z$  784.7) lipids (Table 3 and Fig. 3B, insert). Lithium addition eliminated the presence of sodiated TMHSs, which would co-elute with protonated species of phospholipids (Table 2); thus, lithiated TMHSs can be easily detected in the presence of lithiated PCs, PEs, MMPEs, and DMPEs without the need for high mass resolution (Table 3). Additionally, the product ion spectra of peaks at  $m/z$  770.7 and 784.7 showed neutral losses of 74 and 87 mass units; therefore, we decided to explore the use of neutral-loss scans of 74 mass units. This MS-MS transition revealed an interesting pattern formed by ions at  $m/z$  742.6, 744.6, 756.6, 758.6, 770.6, 784.6, and 798.7 (Fig. 3C). These ions matched the calculated  $m/z$  values for  $[M+Li]^+$  ions of TMHSs with FA compositions of 34:2, 34:1, 35:2, 35:1, 36:2, 37:2, and 38:2, respectively (Table 3).

In summary, this work applied for the first time the principles of shotgun lipidomics to the analysis of three non-

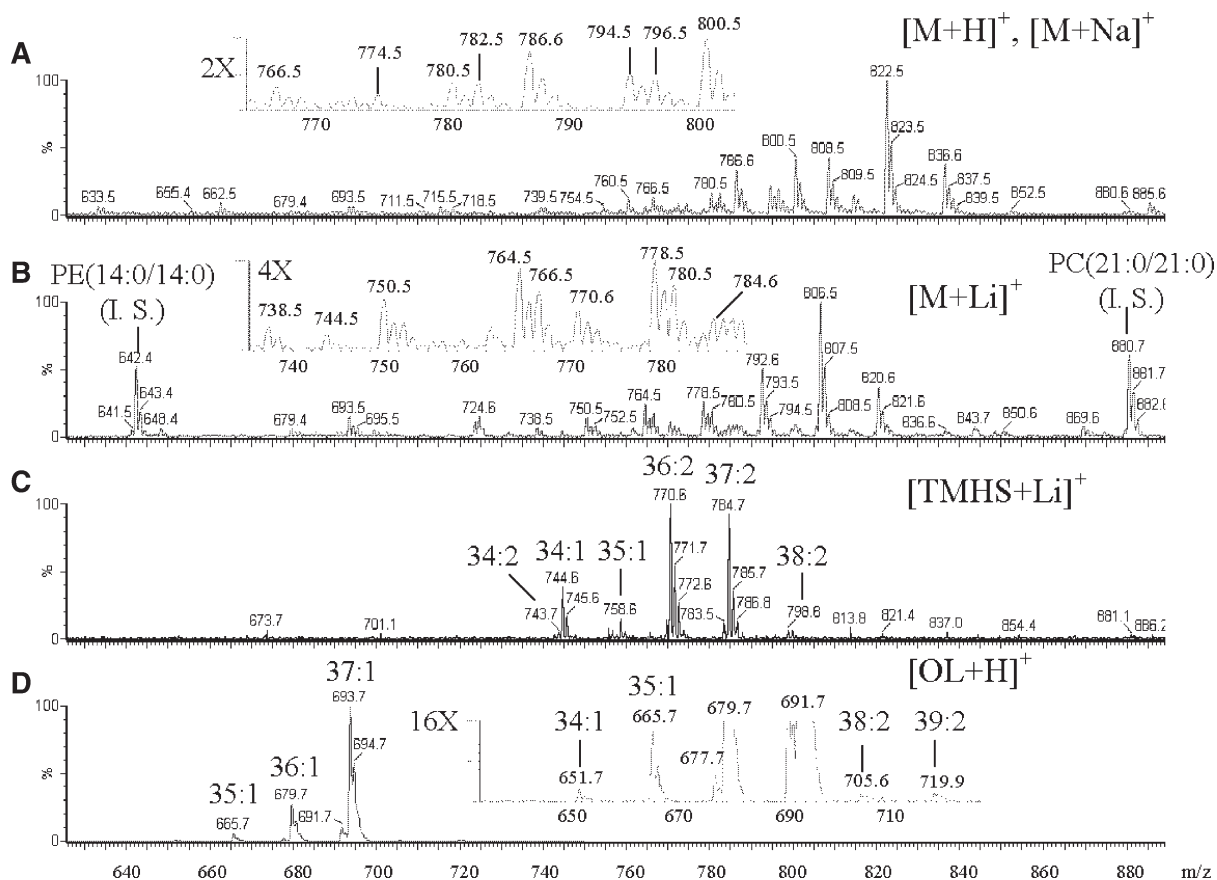


**Fig. 3.** Positive-ion electrospray ionization mass spectra of crude lipid extracts of *S. meliloti* P110 grown under  $P_i$ -starvation conditions. A: Full-scan mode spectrum with no LiCl added. B: Full-scan mode spectrum with 10 mM LiCl added. C: Neutral-loss scan of 74 mass units selective for TMHS. D: Precursor ion scan of  $m/z$  115 selective for OLs. OL, ornithine lipid; PE, phosphatidylethanolamine; PC, phosphatidylcholine; TMHS, 1,2-diacylglycerol-3-*O*-4'-*(N,N,N*-trimethyl)-homoserine lipid.

phosphorus-containing lipid classes. This approach provided for the first time complete FA distributions for these lipid classes using a simple and rapid strategy that did not require chromatography.

#### FA distributions within lipid classes in *S. meliloti*: effects of $P_i$ starvation

The FA distributions for eight lipid classes in *S. meliloti*, including phospholipids and non-phosphorus-containing lipids, were obtained directly from crude extracts under normal conditions (2 mM  $P_i$ ) and under  $P_i$  starvation (Table 4). Analytical and biological variances were of 2–4% for abundant lipids (e.g., PC-36:2 and PG-36:2) when three cultures were analyzed, each one in triplicate, over a period of 1 year. The detection limits for PC, PE, and PG in the MS-MS mode were in the low picomole range (0.5–1.3 pmol/ $\mu$ l). Note that detection limits for a given lipid class will be a function of the MS-MS transition and CEs used for their analysis.

The relative percentage compositions of individual molecular species within lipid classes were obtained using peak areas normalized to the peak area of the internal standard in precursor ion or neutral-loss spectra. The accurate quantitation of phospholipids by ESI-MS is not a simple task, because response factors vary among lipid classes and depend

on the type of MS-MS transition used (42). Additionally, response factors vary within a given lipid class with the length of the fatty acyl chains and number of double bonds (43). The use of diluted lipid solutions and the inclusion of two or more internal standards per lipid class have been recommended to minimize the variability of response factors across lipid classes and within lipid classes (21, 43). We used one internal standard per lipid class, which is acceptable for most applications (44). Our technique is appropriate as a screening method for large volumes of samples when control samples (wild type) are compared with treated samples (wild type in different growth conditions or mutants).

This is the first work to describe FA distributions within lipid classes in *S. meliloti*, for both phospholipids and non-phosphorus-containing lipids. The FA profiles of PEs, MMPEs, DMPEs, and PCs were very similar where 36:2 lipids were the most abundant components (45–60%). Lipids with FA composition 36:2 contained two fatty acyl chains of *cis*-11-octadecenoic acid, which is the most abundant FA in *S. meliloti* membranes (29). The similarity in the FA distributions in these lipid classes is not surprising, because they are closely related biosynthetically (45). SLs on the other hand, showed different FA distributions given by the presence of abundant species that contained hexadecanoic and hexadecenoic acid (32:1 and 32:0). Lipids with FA compo-



TABLE 4. FA distributions in eight lipid classes in *S. meliloti* under normal growth conditions (with 2 mM P<sub>i</sub>) and under P<sub>i</sub>-starvation conditions (with 0 mM P<sub>i</sub>)

Lipid	PCs	PEs	MMPEs	DMPEs	PGs	SLs	TMHSs	OLs
With 2 mM P <sub>i</sub>								
32:1					0.5 ± 0.3	3.2 ± 0.9		
32:0					1.5 ± 0.3	17.8 ± 0.8		
34:2	0.8 ± 0.2	2.8 ± 1.2	1.8 ± 0.4	2.9 ± 1.5	1.9 ± 0.3	1.5 ± 0.4		
34:1	8.0 ± 1.2	19.5 ± 2.9	13.9 ± 1.7	8.7 ± 3.1	28.9 ± 2.8	33.6 ± 2.0		1.2 ± 0.2
35:2	2.5 ± 0.4	2.7 ± 1.6	2.9 ± 0.9		2.1 ± 0.4	1.4 ± 0.5		
35:1	3.0 ± 0.3	3.8 ± 1.8	3.4 ± 0.8		2.6 ± 0.4	4.9 ± 0.6		3.1 ± 0.8
36:2	45.6 ± 2.1	59.0 ± 2.6	56.8 ± 3.4	59.0 ± 2.6	55.5 ± 2.4	17.9 ± 1.5		3.0 ± 0.8
36:1						9.8 ± 2.0		37.0 ± 2.4
37:2	36.0 ± 0.6	11.8 ± 2.0	19.7 ± 1.4	23.2 ± 1.6	6.8 ± 0.6	9.7 ± 1.3		5.3 ± 0.3
37:1								49.6 ± 1.2
38:2	4.2 ± 0.6	0.2 ± 0.3	1.6 ± 0.4	6.1 ± 1.8	0.2 ± 0.2	0.2 ± 0.3		0.6 ± 0.2
39:2								0.2 ± 0.2
With 0 mM P <sub>i</sub>								
32:1						3.4 ± 0.8		
32:0						12.6 ± 3.0		
34:2	0.5 ± 0.4	2.4 ± 1.3	0.8 ± 0.9	1.9 ± 2.2	1.1 ± 0.5	0.9 ± 0.3	1.0 ± 1.1	
34:1	4.9 ± 1.8	11.0 ± 4.5	8.6 ± 4.3	3.3 ± 4.5	15.8 ± 4.3	25.5 ± 2.9	12.8 ± 2.9	1.0 ± 0.1
35:2	2.6 ± 0.6	3.7 ± 1.0	3.4 ± 1.1		3.2 ± 0.9	2.5 ± 0.1	1.6 ± 2.0	
35:1	5.3 ± 1.2	3.5 ± 1.5	5.1 ± 1.3		3.9 ± 0.9	12.2 ± 1.3	2.0 ± 2.4	3.6 ± 0.2
36:2	24.1 ± 2.8	49.9 ± 2.5	45.0 ± 2.5	39.3 ± 3.2	55.2 ± 1.5	7.5 ± 0.6	55.7 ± 6.9	2.9 ± 0.5
36:1						5.2 ± 0.3		23.3 ± 0.4
37:2	49.1 ± 1.8	23.1 ± 7.0	33.3 ± 7.8	41.1 ± 8.8	19.6 ± 4.9	26.9 ± 5.1	25.2 ± 5.0	8.3 ± 0.2
37:1								60.2 ± 0.2
38:2	13.5 ± 3.7	0.9 ± 1.0	3.5 ± 1.1	14.4 ± 1.9	1.2 ± 0.5	3.3 ± 1.3	1.6 ± 2.1	0.4 ± 0.1
39:2								0.4 ± 0.1

Data are given as mean ± SD (n = 6).

sitions of 32:1 and 32:0 were not detected for phospholipids (PEs, MMPEs, DMPEs, PCs). Overall, lipids that contained either 16:1(9) or 16:0 FAs (34:2 and 34:1) were not abundant in phospholipids. PGs are most likely the closest lipid class to SLs from a biosynthetic and biological point of view (46). Lipids that contained 16:1(9) and 16:0 were detected in PGs; however, these species were minor components (2%). Interestingly, hexadecanoic acid was also the most abundant FA found in SLs in other organisms (47, 48).

PCA of FA distributions in lipid classes showed from a schematic point of view a biosynthetic relationship among

lipid classes (Fig. 4A). SLs were a distinctive class, whereas phospholipids were spatially arranged following their biosynthetic order as PGs, PEs, MMPEs, DMPEs, and PCs. PCA of FA distributions in lipid classes under P<sub>i</sub> starvation conditions also showed an interesting pattern (Fig. 4B). The FA distributions in OLs were strikingly different from those of all other lipid classes; this was not unexpected, because of the different biosynthetic origin of OLs (38). However, TMHSs, a distinctive lipid class synthesized exclusively under P<sub>i</sub> starvation, showed profiles that were highly similar to those of phospholipids (Fig. 4B).

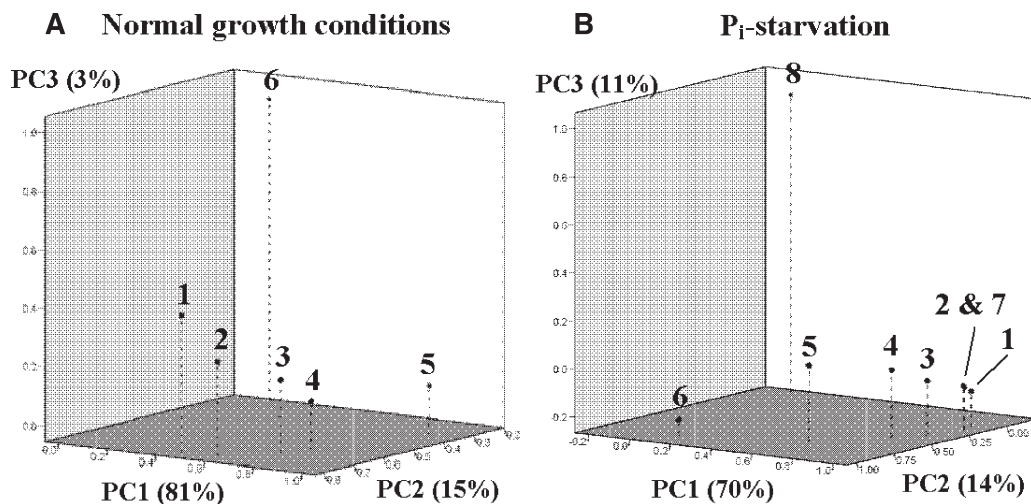


Fig. 4. Principal component analysis of relative percentage composition in lipids of *S. meliloti* P110 under normal growth conditions (A) and under P<sub>i</sub>-starvation conditions (B). Lipid classes are represented by numbers: 1, PGs; 2, PEs; 3, MMPEs; 4, DMPEs; 5, PCs; 6, SLs; 7, TMHs; 8, OLs.

Under  $P_i$  starvation, a significant increase in lipids that contained cyclopropane FAs in all lipid classes was observed (49). Lipids that contained *cis*-9,10-methylenehexadecanoic acid and *cis*-11,12-methyleneoctadecanoic acid (35:2, 35:1, 37:2, 38:2) increased considerably (Table 4). OLS with FA compositions of 37:2 and 37:1 increased significantly under  $P_i$  starvation; therefore it is most likely that these lipids contain cyclopropane FAs.

#### FA distributions within lipid classes in *PhoB*-deficient mutants

The regulator *PhoB* protein is only expressed under  $P_i$ -limiting conditions (8); thus, not surprisingly, the lipid profiles of cultures of *phoB* mutant and wild type were identical under normal ( $P_i$  excess) growth conditions (data not shown). Analysis of total FAs was conducted as a technique complementary to intact lipid analyses (29). Total FA composition of *phoB* mutant and wild type was also identical under normal growth conditions (Table 5). The increased cyclopropanation of lipids observed in the wild type under  $P_i$  starvation was reflected in total FA composition by a significant increase of *cis*-11,12-methyleneoctadecanoic acid (Table 5). Furthermore, a dramatic (73–80%) increase in poly(3-hydroxybutyrate) (PHB) was detected under  $P_i$ -starvation conditions in the wild type (data not shown). However, the increased levels of PHB were not a *PhoB*-dependent response, inasmuch as mutants deficient in the *PhoB* regulator protein also showed increased levels of PHB (data not shown). The cellular role of PHB is not clear, although it has been shown to protect the cell from a diversity of stressors (50, 51).

Under  $P_i$ -limiting conditions, the lipid profiles of *phoB* mutants were different from those of the wild type, as expected (Fig. 5). The biosynthesis of TMHSs in *S. meliloti* is *PhoB*-regulated, inasmuch as *PhoB*-deficient mutants failed to produce these lipids (25). Using the shotgun lipidomics methodology presented in this work, TMHSs were not detected in *PhoB*-deficient mutants grown under  $P_i$  starvation (Fig. 5). Peaks detected at  $m/z$  770.5 and 784.6 for lithiated TMHS-36:2 and TMHS-37:2 lipids, respectively, were not observed in lipid extracts of *PhoB* mutants. Furthermore,

neutral-loss scans of 74 or 87 mass units did not provide the TMHS profiles that were observed in wild-type cultures grown under  $P_i$  starvation (Fig. 3C).

The increased cyclopropanation of lipids observed under  $P_i$  starvation in the wild type was more accentuated in *PhoB*-deficient mutants (see PC-38:2 in Fig. 5). This phenomenon was also observed in total FA composition of *PhoB*-deficient mutants (Table 5). Under  $P_i$  starvation, cyclopropane FAs increased an additional 12% in *phoB* mutants in comparison with the wild type. Cyclopropane FAs comprised 50% of total FAs in *phoB* mutants under  $P_i$  starvation. Total cyclopropane FAs have also been observed to increase significantly in *S. meliloti* as a result of increased acidity (49). The extent of lipid cyclopropanation in *phoB* mutants with  $P_i$  starvation was more pronounced than in the wild type under acidic conditions. Increased cyclopropanation of lipids is a stress response observed with  $P_i$  starvation and acidity; however, this effect was intensified in *PhoB*-deficient mutants with  $P_i$  starvation.

## DISCUSSION

Most methods for lipid analysis employ HPLC separation schemes (33, 52–55), and when the separation of lipid classes and their molecular components is desired, a combination of NP-HPLC followed by RP-HPLC is needed (12). The research presented here allowed the analysis of eight lipid classes in crude lipid extracts of *S. meliloti* using a shotgun lipidomics approach. The collection of mass spectrometric techniques described allowed the detection of 58 molecular lipids with little sample preparation and no chromatography. This is the first report to describe FA distributions in lipids and the relative positions of fatty acyl substituents (*sn*-1, *sn*-2) in phospholipids in *S. meliloti*. We also report new mass spectrometric transitions for the analysis of two phospholipid classes (MMPEs and DMPEs) and three nonphospholipid classes (SLs, TMHSs, and OLS). The addition of lithium salts for analyses in positive electrospray ionization afforded simplified lipid profiles by producing only  $[M+Li]^+$  ions and provided unique MS-

TABLE 5. Percentage compositions of total FAs in *S. meliloti* wild type and *phoB* knockout mutant under normal growth conditions and under  $P_i$  starvation

FAs	FA Percentage Compositions			
	2 mM $P_i$		0 mM $P_i$	
	Wild Type	<i>phoB</i> Knockout	Wild Type	<i>phoB</i> Knockout
14:0	0.33 ± 0.03	0.30 ± 0.02 <sup>c</sup>	0.29 ± 0.06 <sup>a</sup>	0.43 ± 0.04 <sup>a,c</sup>
16:0	11.9 ± 1.1	11.8 ± 1.5	10.2 ± 1.0	10.9 ± 1.0
17:0	0.2 ± 0.1	0.23 ± 0.02 <sup>c</sup>	0.25 ± 0.03 <sup>a</sup>	0.43 ± 0.05 <sup>a,c</sup>
18:0	3.5 ± 0.3	4.0 ± 1.0	1.7 ± 0.3 <sup>a</sup>	3.8 ± 0.9 <sup>a</sup>
16:1(9)	0.9 ± 0.2	0.89 ± 0.05 <sup>c</sup>	0.6 ± 0.1	0.5 ± 0.2 <sup>c</sup>
18:1(11)	58.7 ± 2.9 <sup>b</sup>	57.5 ± 4.1 <sup>c</sup>	48.8 ± 2.6 <sup>a,b</sup>	33.4 ± 2.3 <sup>a,c</sup>
17:0cyclo(9,10)	1.7 ± 0.2	1.8 ± 0.3 <sup>c</sup>	1.7 ± 0.1 <sup>a</sup>	2.6 ± 0.1 <sup>a,c</sup>
19:0cyclo(11,12)	22.6 ± 3.9 <sup>b</sup>	23.5 ± 1.7 <sup>c</sup>	36.5 ± 2.7 <sup>a,b</sup>	47.9 ± 2.5 <sup>a,c</sup>

Data are given as mean ± SD (n = 3).

<sup>a</sup> At 0 mM  $P_i$ , mean values of wild type are significantly different from *phoB* mutant ( $P \leq 0.05$ ).

<sup>b</sup> Mean values of wild type with 0 mM  $P_i$  are significantly different from wild type with 2 mM  $P_i$  ( $P \leq 0.05$ ).

<sup>c</sup> Mean values of *phoB* mutant with 0 mM  $P_i$  are significantly different from *phoB* with 2 mM  $P_i$  ( $P \leq 0.05$ ).

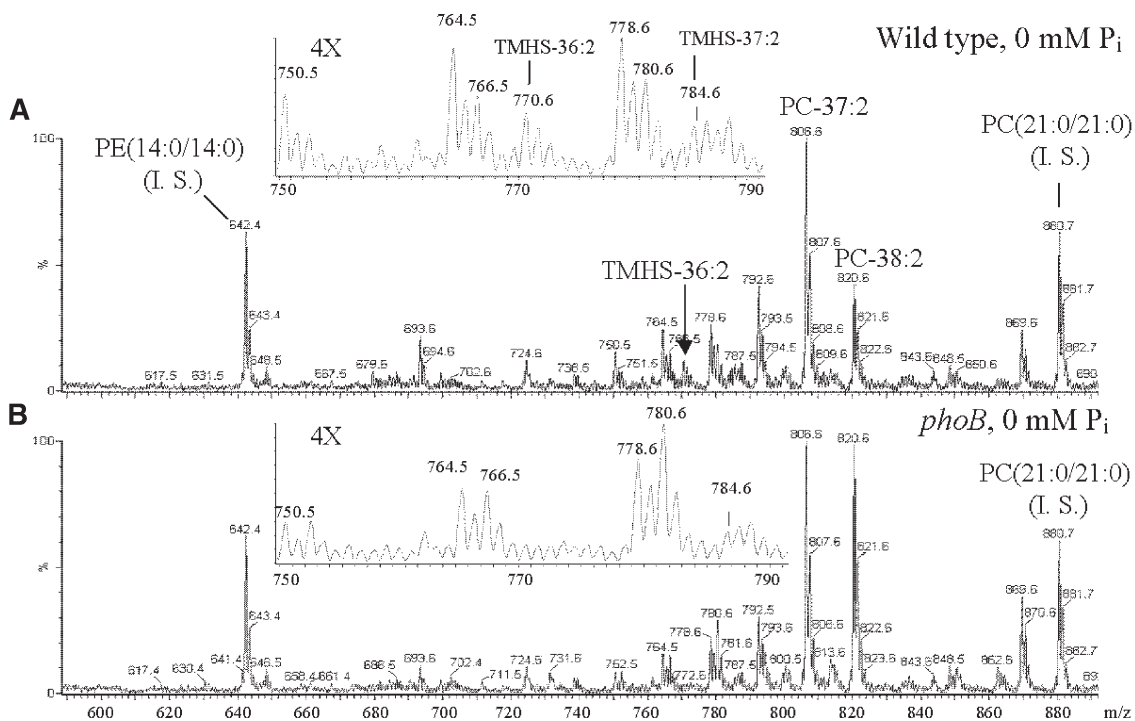


**Fig. 5.** Positive electrospray ionization mass spectra in the full-scan mode of crude lipid extracts of wild type (A) and *phoB* knockout mutant (B) under  $P_i$ -starvation conditions.

MS transitions for each lipid class, which allowed the analysis of isomeric species (PCs, PEs, MMPEs, and DMPEs) with no chromatography. The sensitivity and specificity of these techniques revealed FA distributions for low-abundance lipid classes such as MMPEs, DMPEs, SLs, and OLs in crude bacterial extracts.

This is the first report to use shotgun lipidomics for the analysis of bacterial non-phosphorus-containing lipids such as SLs, TMHSs, and OLs. Normally, the analysis of these lipids requires their isolation via column chromatography or TLC (25, 37, 48, 56–59) and HPLC (60) prior to mass spectrometric detection. FA distributions in these lipid classes are obtained by GC-MS analysis of a chromatographic fraction or TLC spots (47, 48, 56, 61). Typically, these procedures are labor intensive and require milligram amounts of lipids. We demonstrated that profiles for these lipid classes can be obtained from crude extracts using precursor ion scans of  $m/z$  225,  $m/z$  115, and neutral-loss scans of 74 mass units. However, more work needs to be conducted to understand the fragmentation of  $[M+Li]^+$  adducts of TMHSs and  $[M+H]^+$  adducts of OLs in electrospray ionization. This might require the isolation of these lipids by traditional chromatographic techniques due to the unavailability of analytical standards.

Previous lipid analyses of *S. meliloti* using an HPTLC methodology identified nine lipid classes (25). However, complete FA distributions within lipid classes were not revealed using this methodology, inasmuch as only the most abundant molecular components in a lipid class were detected. This is probably a result of poor recoveries of lipids and differential migration of molecular components in TLC plates (16). In our experience, the recoveries of analytical

standards of phospholipids from TLC plates and silica gel columns were lower than when standards or lipid mixtures were infused directly. In contrast to TLC-based protocols that only detected the most abundant molecular species, shotgun lipidomics revealed complete FA distributions within lipid classes, even for low-abundance lipid classes such as OLs and DMPEs (<2%).


Because FA biosynthesis and intact lipid biosynthesis are related and highly coordinated processes, knowledge of FA distributions within lipid classes can provide important clues regarding the biosynthetic origin of lipid classes. The complete FA distributions within lipid classes in *S. meliloti* provided interesting insights into the biosynthetic origin of phospholipids and non-phosphorus-containing lipids. For example, the similarities in FA distributions in TMHSs and phospholipids suggested that TMHSs and phospholipids are synthesized from a common precursor, most likely phosphatidic acid. This was not the case for SLs, which exhibited distinct FA distributions. Therefore, SLs might not be synthesized from the same biochemical precursor as phospholipids and TMHSs. In algae, interestingly, TMHSs and SLs shared the same FA distributions, formed mostly by hexadecanoic acid (48). In contrast, in *S. meliloti*, TMHSs were closer to phospholipids such as PEs rather than to SLs.

Shotgun lipidomics analysis of PhoB-deficient mutants under  $P_i$  starvation confirmed the absence of TMHSs, as demonstrated previously using traditional TLC protocols. Additionally, we found that lipid cyclopropanation increased in PhoB-deficient mutants under  $P_i$  starvation, indicated by a 25% increase in total cyclopropane FAs. The mechanism for the observed increase in cyclopropanation is not clear, because gene expression studies did not show

increased expression of the cyclopropane fatty acyl synthase genes when the cells were grown under P<sub>i</sub>-limiting conditions (49). It appears that lipid cyclopropanation is a general stress response, and in the absence of the PhoB regulator, cells are unable to manage stress caused by P<sub>i</sub> limitation and therefore are under increased stress.

The shotgun lipidomics approach presented here is a rapid and simple strategy for the screening of large volumes of samples in functional genomics studies. Lipid extracts were prepared from 50 ml of bacterial cultures; however, only 1/20 of samples (≈1–2 mg of wet cells, equivalent to 3 ml of bacterial culture) were used for analyses. Furthermore, good signal-to-noise ratios were obtained when 10-fold less material was used (0.3 ml of culture). Thus, complete analyses can be conducted with small sample amounts. The analysis time per sample (about 60 min) was shorter than the time required by most HPLC procedures (52, 55).

The absolute quantitation of lipids was not achieved in this research. However, this method is suitable for those studies in which a stressed (mutant strain) sample is compared with a control (wild-type strain) sample. The absolute quantitation of lipids remains a future objective of this work, and, therefore, more efforts are required in this area. The quantitation of bacterial non-phosphorus-containing lipids using shotgun lipidomics remains a challenge, inasmuch as analytical standards of these lipids are not available.

One disadvantage of the shotgun lipidomics methodology presented here is that CLs were not detected in crude extracts of *S. meliloti*. CLs have been successfully analyzed as their [M-2H]<sup>2-</sup> ions with shotgun lipidomics approaches using precursor ion scans of *m/z* 153; no evidence of ion suppression was observed (21, 62, 63). We were not able to detect these lipids in crude lipid extracts using precursor ion scans of *m/z* 153. Because CLs are a minor lipid class in *S. meliloti*, it is possible that these lipids coeluted with PEs or PGs in negative electrospray ionization. 

## REFERENCES

- Jones, K. M., H. Kobayashi, B. W. Davies, M. E. Taga, and G. C. Walker. 2007. How rhizobial symbionts invade plants: the Sinorhizobium-Medicago model. *Nat. Rev. Microbiol.* **5**: 619–633.
- Lodwig, E., and P. Poole. 2003. Metabolism of Rhizobium bacteroids. *Crit. Rev. Plant Sci.* **22**: 37–78.
- Galibert, F., T. M. Finan, S. R. Long, A. Puhler, P. Abola, F. Ampe, F. Barloy-Hubler, M. J. Barnett, A. Becker, P. Boistard, et al. 2001. The composite genome of the legume symbiont *Sinorhizobium meliloti*. *Science*. **293**: 668–672.
- Garg, N. and Geetanjali. 2007. Symbiotic nitrogen fixation in legume nodules: process and signaling. A review. *Agron. Sustain. Dev.* **27**: 59–68.
- Colebatch, G., B. Trevaskis, and M. Udvardi. 2002. Symbiotic nitrogen fixation research in the postgenomics era. *New Phytol.* **153**: 37–42.
- MacLean, A. M., T. M. Finan, and M. J. Sadowsky. 2007. Genomes of the symbiotic nitrogen-fixing bacteria of legumes. *Plant Physiol.* **144**: 615–622.
- Weidner, S., A. Puhler, and H. Kuster. 2003. Genomics insights into symbiotic nitrogen fixation. *Curr. Opin. Biotechnol.* **14**: 200–205.
- Yuan, Z. C., R. Zaheer, R. Morton, and T. M. Finan. 2006. Genome prediction of PhoB regulated promoters in *Sinorhizobium meliloti* and twelve proteobacteria. *Nucleic Acids Res.* **34**: 2686–2697.
- German, J. B., L. A. Gillies, J. T. Smilowitz, A. M. Zivkovic, and S. M. Watkins. 2007. Lipidomics and lipid profiling in metabolomics. *Curr. Opin. Lipidol.* **18**: 66–71.
- Watson, A. D. 2006. Lipidomics: a global approach to lipid analysis in biological systems. *J. Lipid Res.* **47**: 2101–2111.
- Wenk, M. R. 2005. The emerging field of lipidomics. *Nat. Rev. Drug Discov.* **4**: 594–610. [Erratum. 2005. *Nat. Rev. Drug Discov.* **4**: 725.]
- Peterson, B. L., and B. S. Cummings. 2006. A review of chromatographic methods for the assessment of phospholipids in biological samples. *Biomed. Chromatogr.* **20**: 227–243.
- Tranchida, P., P. Donato, P. Dugo, G. Dugo, and L. Mondello. 2007. Comprehensive chromatographic methods for the analysis of lipids. *Trends Analyt. Chem.* **26**: 191–205.
- Gao, F., J. Dong, W. Li, T. Wang, H. Liao, Y. P. Liao, and H. W. Liu. 2006. Separation of phospholipids by capillary zone electrophoresis with indirect ultraviolet detection. *J. Chromatogr. A.* **1130**: 259–264.
- Christie, W. W. 2003. Lipid Analysis. 3<sup>rd</sup> edition. The Oily Press Lipid Library, Bridgewater. 137–180.
- Delong, C. J., P. R. Baker, M. Samuel, Z. Cui, and M. J. Thomas. 2001. Molecular species composition of rat liver phospholipids by ESI-MS/MS: the effect of chromatography. *J. Lipid Res.* **42**: 1959–1968.
- Houjou, T., K. Yamatani, M. Imagawa, T. Shimizu, and R. Taguchi. 2005. A shotgun tandem mass spectrometric analysis of phospholipids with normal-phase and/or reverse-phase liquid chromatography/electrospray ionization mass spectrometry. *Rapid Commun. Mass Spectrom.* **19**: 654–666.
- Pulfer, M., and R. C. Murphy. 2003. Electrospray mass spectrometry of phospholipids. *Mass Spectrom. Rev.* **22**: 332–364.
- Han, X., and R. W. Gross. 2003. Global analyses of cellular lipidomes directly from crude extracts of biological samples by ESI mass spectrometry: a bridge to lipidomics. *J. Lipid Res.* **44**: 1071–1079.
- Han, X., and R. W. Gross. 2005. Shotgun lipidomics: multidimensional MS analysis of cellular lipidomes. *Expert Rev. Proteomics.* **2**: 253–264.
- Han, X., and R. W. Gross. 2005. Shotgun lipidomics: electrospray ionization mass spectrometric analysis and quantitation of cellular lipidomes directly from crude extracts of biological samples. *Mass Spectrom. Rev.* **24**: 367–412.
- Hsu, F. F., and J. Turk. 2000. Characterization of phosphatidylethanolamine as a lithiated adduct by triple quadrupole tandem mass spectrometry with electrospray ionization. *J. Mass Spectrom.* **35**: 595–606.
- Hsu, F. F., and J. Turk. 2001. Studies on phosphatidylglycerol with triple quadrupole tandem mass spectrometry with electrospray ionization: fragmentation processes and structural characterization. *J. Am. Soc. Mass Spectrom.* **12**: 1036–1043.
- Hsu, F. F., and J. Turk. 2003. Electrospray ionization/tandem quadrupole mass spectrometric studies on phosphatidylcholines: the fragmentation processes. *J. Am. Soc. Mass Spectrom.* **14**: 352–363.
- Geiger, O., V. Rohrs, B. Weissenmayer, T. M. Finan, and J. E. Thomas-Oates. 1999. The regulator gene *phoB* mediates phosphate stress-controlled synthesis of the membrane lipid diacylglycerol-N, N,N-trimethylhomoserine in Rhizobium (*Sinorhizobium*) *meliloti*. *Mol. Microbiol.* **32**: 63–73.
- Summers, M. L., J. G. Elkins, B. A. Elliott, and T. R. McDermott. 1998. Expression and regulation of phosphate stress inducible genes in *Sinorhizobium meliloti*. *Mol. Plant Microbe Interact.* **11**: 1094–1101.
- Bardin, S. D., and T. M. Finan. 1998. Regulation of phosphate assimilation in Rhizobium (*Sinorhizobium*) *meliloti*. *Genetics.* **148**: 1689–1700.
- Bardin, S., S. Dan, M. Osteras, and T. M. Finan. 1996. A phosphate transport system is required for symbiotic nitrogen fixation by *Rhizobium meliloti*. *J. Bacteriol.* **178**: 4540–4547.
- Basconcillo, L. S., and B. E. McCarry. 2008. Comparison of three GC/MS methodologies for the analysis of fatty acids in *Sinorhizobium meliloti*: development of a micro-scale, one-vial method. *J. Chromatogr. B Analyt. Technol. Biomed. Life Sci.* **871**: 22–31.
- Hsu, F. F., A. Bohrer, and J. Turk. 1998. Formation of lithiated adducts of glycerophosphocholine lipids facilitates their identification by electrospray ionization tandem mass spectrometry. *J. Am. Soc. Mass Spectrom.* **9**: 516–526.
- Griffiths, W. J. 2003. Tandem mass spectrometry in the study of fatty acids, bile acids, and steroids. *Mass Spectrom. Rev.* **22**: 81–152.
- Hsu, F. F., J. Turk, T. D. Williams, and R. Welti. 2007. Electrospray ionization multiple stage quadrupole ion-trap and tandem quadrupole mass spectrometric studies on phosphatidylglycerol from Arabidopsis leaves. *J. Am. Soc. Mass Spectrom.* **18**: 783–790.
- Oursel, D., C. Loutelier-Bourhis, N. Orange, S. Chevalier, V. Norris, and C. M. Lange. 2007. Lipid composition of membranes of *Escherichia*

- coli* by liquid chromatography/tandem mass spectrometry using negative electrospray ionization. *Rapid Commun. Mass Spectrom.* **21**: 1721–1728.
34. Taoka, Y., S. Ishioka, and Y. Itabashi. 2005. Molecular species analysis of phosphatidylglycerols in *Escherichia coli* by reversed-phase HPLC/ESI-MS. *Bunseki Kagaku.* **54**: 155–160.
35. Murphy, R. C., J. Fiedler, and J. Hevko. 2001. Analysis of nonvolatile lipids by mass spectrometry. *Chem. Rev.* **101**: 479–526.
36. Cedergren, R. A., and R. I. Hollingsworth. 1994. Occurrence of sulfoquinovosyl diacylglycerol in some members of the family Rhizobiaceae. *J. Lipid Res.* **35**: 1452–1461.
37. Ishizuka, I. 1997. Chemistry and functional distribution of sulfoglycolipids. *Prog. Lipid Res.* **36**: 245–319.
38. Gao, J. L., B. Weissenmayer, A. M. Taylor, J. Thomas-Oates, I. M. Lopez-Lara, and O. Geiger. 2004. Identification of a gene required for the formation of lyso-ornithine lipid, an intermediate in the biosynthesis of ornithine-containing lipids. *Mol. Microbiol.* **53**: 1757–1770.
39. Choma, A., and I. Komanecka. 2002. Analysis of phospholipids and ornithine-containing lipids from *Mesorhizobium* spp. *Syst. Appl. Microbiol.* **25**: 326–331.
40. Dembitsky, V. M. 1996. Betaine ether-linked glycerolipids: chemistry and biology. *Prog. Lipid Res.* **35**: 1–51.
41. Lopez-Lara, I. M., J. L. Gao, M. J. Soto, A. Solares-Perez, B. Weissenmayer, C. Sohlenkamp, G. P. Verroios, J. Thomas-Oates, and O. Geiger. 2005. Phosphorus-free membrane lipids of *Sinorhizobium meliloti* are not required for the symbiosis with alfalfa but contribute to increased cell yields under phosphorus-limiting conditions of growth. *Mol. Plant Microbe Interact.* **18**: 973–982.
42. Han, X., K. Yang, J. Yang, K. N. Fikes, H. Cheng, and R. W. Gross. 2006. Factors influencing the electrospray intrasource separation and selective ionization of glycerophospholipids. *J. Am. Soc. Mass Spectrom.* **17**: 264–274.
43. Koivusalo, M., P. Haimi, L. Heikinheimo, R. Kostiaainen, and P. Somerharju. 2001. Quantitative determination of phospholipid compositions by ESI-MS: effects of acyl chain length, unsaturation, and lipid concentration on instrument response. *J. Lipid Res.* **42**: 663–672.
44. Zacarias, A., D. Bolanowski, and A. Bhatnagar. 2002. Comparative measurements of multicomponent phospholipid mixtures by electrospray mass spectroscopy: relating ion intensity to concentration. *Anal. Biochem.* **308**: 152–159.
45. Lopez-Lara, I. M., C. Sohlenkamp, and O. Geiger. 2003. Membrane lipids in plant-associated bacteria: their biosyntheses and possible functions. *Mol. Plant Microbe Interact.* **16**: 567–579.
46. Frentzen, M. 2004. Phosphatidylglycerol and sulfoquinovosyldiacylglycerol: anionic membrane lipids and phosphate regulation. *Curr. Opin. Plant Biol.* **7**: 270–276.
47. Ben Hamed, K., N. Ben Youssef, A. Ranieri, M. Zarrouk, and C. Abdely. 2005. Changes in content and fatty acid profiles of total lipids and sulfolipids in the halophyte *Crithmum maritimum* under salt stress. *J. Plant Physiol.* **162**: 599–602.
48. Sanina, N. M., S. N. Goncharova, and E. Y. Kostetsky. 2004. Fatty acid composition of individual polar lipid classes from marine macrophytes. *Phytochemistry.* **65**: 721–730.
49. Basconcello, L. S., R. Zaheer, T. M. Finan, and B. E. McCarty. 2009. Cyclopropane fatty acyl synthase in *Sinorhizobium meliloti*. *Microbiology-Ük.* **155**: 373–385.
50. Trainer, M. A., and T. C. Charles. 2006. The role of PHB metabolism in the symbiosis of rhizobia with legumes. *Appl. Microbiol. Biotechnol.* **71**: 377–386.
51. Wang, C., M. Saldanha, X. Sheng, K. J. Shelswell, K. T. Walsh, B. W. Sobral, and T. C. Charles. 2007. Roles of poly-3-hydroxybutyrate (PHB) and glycogen in symbiosis of *Sinorhizobium meliloti* with *Medicago* sp. *Microbiology.* **153**: 388–398.
52. Bang, D. Y., E. J. Ahn, and M. H. Moon. 2007. Shotgun analysis of phospholipids from mouse liver and brain by nanoflow liquid chromatography/tandem mass spectrometry. *J. Chromatogr. B Analyt. Technol. Biomed. Life Sci.* **852**: 268–277.
53. Hayakawa, J., T. Ono, K. Hanasaki, and Y. Okabayashi. 2006. Simultaneous quantitative analysis for phospholipids in human HDL and LDL using two internal standards by liquid chromatography/mass spectrometry. *Anal. Lett.* **39**: 957–972.
54. Rainville, P. D., C. L. Stumpf, J. P. Shockcor, R. S. Plumb, and J. K. Nicholson. 2007. Novel application of reversed-phase UPLC-oeTOF-MS for lipid analysis in complex biological mixtures: a new tool for lipidomics. *J. Proteome Res.* **6**: 552–558.
55. Taguchi, R., J. Hayakawa, Y. Takeuchi, and M. Ishida. 2000. Two-dimensional analysis of phospholipids by capillary liquid chromatography/electrospray ionization mass spectrometry. *J. Mass Spectrom.* **35**: 953–966.
56. de Souza, L. M., M. Iacomini, P. A. Gorin, R. S. Sari, M. A. Haddad, and G. L. Sasaki. 2007. Glyco- and sphingophospholipids from the medusa *Phyllorhiza punctata*: NMR and ESI-MS/MS fingerprints. *Chem. Phys. Lipids.* **145**: 85–96.
57. Kato, M., K. Hajiro Nakanishi, H. Sano, and S. Miyachi. 1995. Polyunsaturated fatty acids and betaine lipids from *Pavlova lutheri*. *Plant Cell Physiol.* **36**: 1607–1611.
58. Naumann, I., K. H. Darsow, C. Walter, H. A. Lange, and R. Buchholz. 2007. Identification of sulfoacyl lipids from the alga *Porphyridium purpureum* by matrix-assisted laser desorption/ionisation quadrupole ion trap time-of-flight mass spectrometry. *Rapid Commun. Mass Spectrom.* **21**: 3185–3192.
59. Weissenmayer, B., O. Geiger, and C. Benning. 2000. Disruption of a gene essential for sulfoquinovosyldiacylglycerol biosynthesis in *Sinorhizobium meliloti* has no detectable effect on root nodule symbiosis. *Mol. Plant Microbe Interact.* **13**: 666–672.
60. Norman, H. A., C. F. Mischke, B. Allen, and J. S. Vincent. 1996. Semi-preparative isolation of plant sulfoquinovosyldiacylglycerols by solid phase extraction and HPLC procedures. *J. Lipid Res.* **37**: 1372–1376.
61. Berge, J. P., E. Debiton, J. Dumay, P. Durand, and C. Barthomeuf. 2002. In vitro anti-inflammatory and anti-proliferative activity of sulfolipids from the red alga *Porphyridium cruentum*. *J. Agric. Food Chem.* **50**: 6227–6232.
62. Han, X., K. Yang, J. Yang, H. Cheng, and R. W. Gross. 2006. Shotgun lipidomics of cardiolipin molecular species in lipid extracts of biological samples. *J. Lipid Res.* **47**: 864–879.
63. Hsu, F. F., J. Turk, E. R. Rhoades, D. G. Russell, Y. X. Shi, and E. A. Groisman. 2005. Structural characterization of cardiolipin by tandem quadrupole and multiple-stage quadrupole ion-trap mass spectrometry with electrospray ionization. *J. Am. Soc. Mass Spectrom.* **16**: 491–504.